Liquid Crystals
Publication details, including instructions for authors and subscription information:
http://www.informaworld.com/smpp/title~content=t713926090

Shear flow and magnetic field effects on smectic C, C*, C_M and C^*_M liquid crystals

S. P. A. Gill[a]; F. M. Leslie[a]
[a] Department of Mathematics, University of Strathclyde, Glasgow, Scotland

To cite this Article Gill, S. P. A. and Leslie, F. M.(1993) 'Shear flow and magnetic field effects on smectic C, C*, C_M and C^*_M liquid crystals', Liquid Crystals, 14: 6, 1905 — 1923
To link to this Article: DOI: 10.1080/02678299308027727
URL: http://dx.doi.org/10.1080/02678299308027727

LIQUID CRYSTALS, 1993, VOL. 14, NO. 6, 1905–1923

Shear flow and magnetic field effects on smectic C, C*, C_M and C_M^* liquid crystals

by S. P. A. GILL and F. M. LESLIE*
Department of Mathematics, University of Strathclyde, Livingstone Tower, Richmond Street, Glasgow G1 1XH, Scotland

The continuum equations of Leslie *et al.* [1] for smectic C, and the extension of this theory for chiral smectic C* [2], are applied to problems involving simple planar layer configurations which accommodate uniform layer thickness constraints. The chiral smectic C_M^* and non-chiral smectic C_M [3] are considered as either biaxial smectic A phases or antiferroelectric smectic C phases and are therefore included as interesting degenerate cases of the smectic C* and C phases, respectively. The effects of static and time dependent magnetic fields on these materials are compared with related deformations occurring in nematics [4] and cholesterics [5, 6]. Their reaction to applied shears is also investigated yielding examples of flow alignment, induced secondary flows and unwinding of the chiral helix and testing the validity of enforcing a constant layer thickness.

1. Introduction

Recently Leslie *et al.* [1] have proposed a constrained theory for smectic C liquid crystals that may be useful for the analysis of some of the effects in these materials. The theory is based on two simplifying assumptions that clearly restrict its range of applicability. These are that the layers although deformed remain of constant thickness, and also that the angle of tilt of the alignment with respect to the layer normal remains fixed, the former appearing reasonable in many situations, and the latter provided pretransitional and thermal effects are negligible.

Such theory results in a quadratic elastic energy that contains eleven terms for chiral materials [2] and nine for non-chiral smectics [7]. Here, however, our aim is to examine preliminary predictions based on the corresponding dynamic theory. This theory contains twenty dissipative terms in the stress tensor, but nonetheless some progress is possible in discussing the simpler arrangements in shear flow.

The essential difference between the nematic case and the smectic one is the restriction imposed by the layered structure of the smectic. Any shear must be applied parallel to the layers in order to retain any possibility of preserving them. This is a necessary condition but it is not a completely sufficient one. If the anisotropic axes of the smectic molecules are not confined to the plane of shear it is clearly apparent that moving these strata over one another will induce a secondary velocity perpendicular to the plane of shear. If this transverse velocity acts against a boundary an internal pressure will be generated which must inevitably lead to deformation of the layered structure. In this paper shear flow of two differently orientated samples, a planar homeotropic and a bookshelf alignment, are examined to illustrate some of these effects.

* Author for correspondence.

2. A continuum theory for smectics C, C*, C_M and C_M^*

All the smectic phases under consideration are layered, biaxial phases. Smectic C consists of rod-like uniaxial molecules which align at a constant angle of tilt to the layers in an isothermal system. This is a well-documented liquid crystal phase, but probably not so well-known is the smectic C_M phase recently described by Brand and Pleiner [3]. The M subscript acknowledges McMillan who first predicted their existence about 20 years ago although they have only recently been discovered in polymeric liquid crystals. They consist of disc-like biaxial molecules where one axis coincides with the layer normal, which we could describe as a biaxial smectic A phase. It is of interest to note that an antiferroelectric smectic C phase, where the tilted molecules alternate in direction around the layer normal by 180° as we cross each layer, also possesses a similar symmetry to that of smectic C_M and so can be modelled by the same continuum theory.

For all these phases the * superscript denotes the chiral version of the phase in which the molecules rotate with a constant pitch around the layer normal as we cross the layers. This helical structure leads to the presence of a permanent polarization in smectic C* which appears in the plane of the layers perpendicular to the molecules. Any externally applied electric field interacts with this permanent polarization leading to the fast switching mechanism these ferroelectric phases exhibit. However the additional symmetry of smectic C_M^* means that no such permanent polarization is evident in this chiral phase. Therefore, as the ferroelectric behaviour of smectic C* will be markedly different from that of smectic C_M^* in an electric field, we confine our investigations to their responses in magnetic fields.

We start with the continuum model for smectic C derived by Leslie *et al.* [1] which describes the smectic structure by a pair of orthogonal unit vectors **a** and **c**. The vector **a** is the density wave vector which also coincides with the layer normal due to the assumption that the layers have a constant thickness. The second vector **c** is perpendicular to **a** and describes the direction of tilt of the alignment with respect to the layer normal. Geometrical considerations lead to the assumption that any constitutive relations in the model should remain invariant under the changes of sign

$$\mathbf{a} \to -\mathbf{a} \text{ and } \mathbf{c} \to -\mathbf{c}. \tag{2.1}$$

This simultaneous transformation allows terms that are even and odd in multiples of **a** and **c**. However the additional symmetry of the smectic C_M phase implies that we can have an independent change of sign

$$\mathbf{a} \to -\mathbf{a} \text{ or } \mathbf{c} \to -\mathbf{c}. \tag{2.2}$$

In this case only terms involving even multiples of **a** and **c** can exist. Therefore the smectic C_M and C_M^* phases can be modelled using a degenerate case of the smectic C and C* models, respectively. Removing the terms odd in **a** and **c** from the constitutive relations for the elastic energy function and the viscous stress tensor is simply achieved by letting

$$K_4^c = K_i^{ac} = \tau_i = \kappa_i = 0 \text{ for all } i \tag{2.3}$$

in the smectic C continuum theory. The helical phases are modelled by the addition of a chiral term into the elastic energy function which was derived by Carlsson *et al.* [2]. They also predicted a second chiral term, but this is not found to be of importance in the situations investigated here and as there is some doubt about its existence, it is omitted.

In summary we now have the following elastic energy function

$$
\begin{aligned}
2W=&\begin{bmatrix} K_1^a(a_{i,i})^2+K_2^a(c_ia_{i,j}c_j)^2+2K_3^a a_{i,i}(c_ja_{j,k}c_k) \\ +K_1^c(c_{i,i})^2+K_2^c c_{i,j}c_{i,j}+K_3^c c_{i,j}c_jc_{i,k}c_k \end{bmatrix}^{\mathrm{C,C^*,C_M,C_M^*}} \\
&+[2K_4^c c_ic_{k,i}c_{k,q}a_q+2K_1^{ac}c_{i,i}(c_ja_{j,k}c_k)+2K_2^{ac}c_{i,i}a_{j,j}]^{\mathrm{C,C^*}} \\
&-\left[\frac{4\pi K_2^c}{P}\varepsilon_{ijk}a_jc_kc_{i,p}a_p\right]^{\mathrm{C^*,C_M^*}},
\end{aligned}
\tag{2.4}
$$

and viscous stress tensor

$$
\left.
\begin{aligned}
\tilde{t}_{ij}^{s}=&\begin{bmatrix} \mu_0D_{ij}+\mu_1a_pD_p^aa_ia_j+\mu_2(D_i^aa_j+D_j^aa_i)+\mu_3c_pD_p^cc_ic_j \\ +\mu_4(D_i^cc_j+D_j^cc_i)+\mu_5c_pD_p^a(a_ic_j+a_jc_i)+\lambda_1(A_ia_j+A_ja_i) \\ +\lambda_2(C_ic_j+C_jc_i)+\lambda_3c_pA_p(a_ic_j+a_jc_i) \end{bmatrix}^{\mathrm{C,C^*,C_M,C_M^*}} \\
&+\begin{bmatrix} \kappa_1(D_i^ac_j+D_j^ac_i+D_i^ca_j+D_j^ca_i)+\kappa_2a_pD_p^a(a_ic_j+a_jc_i) \\ +2\kappa_2a_pD_p^ca_ia_j+\kappa_3[c_pD_p^c(a_ic_j+a_jc_i)+2a_pD_p^cc_ic_j] \\ +\tau_1(C_ia_j+C_ja_i)+\tau_2(A_ic_j+A_jc_i)+2\tau_3c_pA_pa_ia_j \\ +2\tau_4c_pA_pc_ic_j \end{bmatrix}^{\mathrm{C,C^*}}, \\
\tilde{t}_{ij}^{ss}=&\begin{bmatrix} \lambda_1(D_j^aa_i-D_i^aa_j)+\lambda_2(D_j^cc_i-D_i^cc_j)+\lambda_3c_pD_p^a(a_ic_j-a_jc_i) \\ +\lambda_4(A_ja_i-A_ia_j)+\lambda_5(C_jc_i-C_ic_j)+\lambda_6c_pA_p(a_ic_j-a_jc_i) \end{bmatrix}^{\mathrm{C,C^*,C_M,C_M^*}} \\
&\begin{bmatrix} +\tau_1(D_j^ac_i-D_i^ac_j)+\tau_2(D_j^ca_i-D_i^ca_j)+\tau_3a_pD_p^a(a_ic_j-a_jc_i) \\ +\tau_4c_pD_p^c(a_ic_j-a_jc_i)+\tau_5(A_jc_i-A_ic_j+C_ja_i-C_ia_j) \end{bmatrix}^{\mathrm{C,C^*}},
\end{aligned}
\right\}
\tag{2.5}
$$

where the s and ss superscripts denote the symmetric and skew-symmetric parts of the tensor and the superscripts on the square brackets indicate for which phases the terms inside are relevant.

3. Shear flow of a planar homeotropic sample

The smectic liquid crystal is arranged in horizontal layers between two infinite parallel plates a distance $2d$ apart (see Beresnev *et al.* [8] for a practical method of orientating such samples). The lower one is at rest while the upper one is moved with a velocity U in a straight line in its own plane. The origin is mid-way between the plates with the z axis normal to the plates and the x axis parallel to the direction of motion of the upper plate. The alignment is described by the layer normal **a** which coincides with the z axis and the projection of the director in the x–y plane **c**.

The layer normal **a** is assumed to be constant and the velocity **v** and the c director **c** are assumed to be purely functions of z and are given by

$$\mathbf{a}=[0,0,1],\quad \mathbf{c}=[\cos\phi(z),\sin\phi(z),0],\quad \mathbf{v}=[u(z),v(z),0], \tag{3.1}$$

where ϕ is the angle between $\mathbf{c}$ and the x axis, $u(z)$ is the velocity in the shear plane and $v(z)$ is the secondary velocity.

Investigations of the added effect of the chirality of the helical structures of smectics C* and C^*_M reveals that this has no contribution to the governing equations and simply adds a chiral term to the elastic energy function. The chiral materials are therefore easily described using the non-chiral models with suitably adjusted boundary conditions. For this reason the shear flow behaviour of the chiral smectics C* and C^*_M are considered together with their non-chiral counterparts smectics C and C_M, respectively.

3.1. *Shear flow of smectics C and C**

3.1.1. *The elastic energy function*

The non-chiral contribution to the elastic energy function is due to resistance encountered when rotating the director around the layer normal away from its minimum energy position.

$$W=\tfrac{1}{2}K_2^c[\tfrac{1}{2}(\mathbf{b}\cdot\nabla\times\mathbf{b}+\mathbf{c}\cdot\nabla\times\mathbf{c})]^2=\tfrac{1}{2}K_2^c\left(\frac{d\phi}{dz}\right)^2, \quad \mathbf{b}=\mathbf{a}\times\mathbf{c}. \tag{3.1.1}$$

The chiral term arises from a similar distortion but plays no part in the governing equations

$$W^*=K_2^c q[\tfrac{1}{2}(\mathbf{b}\cdot\nabla\times\mathbf{b}+\mathbf{c}\cdot\nabla\times\mathbf{c})]=-K_2^c q\frac{d\phi}{dz}, \tag{3.1.2}$$

where $q=2\pi/P$ is the wave vector of the pitch P. The discussion of the statics of these smectics by Carlsson *et al.* [9] suggests that K_2^c be positive.

3.1.2. *The linear momentum balance*

In the absence of applied pressure gradients and external body forces and couples, and adopting the Onsager viscosity relations we have

$$\left.\begin{aligned}\frac{d(\tilde{t}_{xz})}{dz}&=\frac{d}{dz}\left[\eta_1\frac{du}{dz}+\eta_2\left(\frac{du}{dz}\cos\phi+\frac{dv}{dz}\sin\phi\right)\cos\phi\right]=0,\\ \frac{d(\tilde{t}_{yz})}{dz}&=\frac{d}{dz}\left[\eta_1\frac{dv}{dz}+\eta_2\left(\frac{du}{dz}\cos\phi+\frac{dv}{dz}\sin\phi\right)\sin\phi\right]=0,\end{aligned}\right\} \tag{3.1.3}$$

in the x and y directions, respectively, where the η_i are the following combinations of viscosity coefficients

$$\left.\begin{aligned}\eta_1&=\tfrac{1}{2}(\mu_0+\mu_2-2\lambda_1+\lambda_4),\\ \eta_2&=\tfrac{1}{2}(\mu_4+\mu_5+2\lambda_2-2\lambda_3+\lambda_5+\lambda_6).\end{aligned}\right\} \tag{3.1.4}$$

These equations can both be integrated once with respect to z to give

$$\tilde{t}_{xz}=\eta_1\frac{du}{dz}+\eta_2\left(\frac{du}{dz}\cos\phi+\frac{dv}{dz}\sin\phi\right)\cos\phi=c_1, \tag{3.1.5}$$

$$\tilde{t}_{yz}=\eta_1\frac{dv}{dz}+\eta_2\left(\frac{du}{dz}\cos\phi+\frac{dv}{dz}\sin\phi\right)\sin\phi=c_2, \tag{3.1.6}$$

which leads to the appearance of c_1 and c_2, the shearing forces per unit area in the x and y directions, respectively. On rearrangement we have expressions for the velocity components $u(z)$ and $v(z)$.

$$\frac{du}{dz}=\frac{c_1(\eta_1+\eta_2\sin^2\phi)-c_2\eta_2\sin\phi\cos\phi}{\eta_1(\eta_1+\eta_2)}, \tag{3.1.7}$$

$$\frac{dv}{dz}=\frac{c_2(\eta_1+\eta_2\cos^2\phi)-c_1\eta_2\sin\phi\cos\phi}{\eta_1(\eta_1+\eta_2)}. \tag{3.1.8}$$

3.1.3. *The angular momentum balance*

The angular momentum c equations yield

$$K_2^c\frac{d^2\phi}{dz^2}+(\tau_1-\tau_5)\left(\frac{du}{dz}\sin\phi-\frac{dv}{dz}\cos\phi\right)=0, \tag{3.1.9}$$

or, substituting equation (3.1.1) and equations (3.1.7) and (3.1.8) we obtain

$$\frac{dW}{d\phi}=\tilde{t}_{xy}-\tilde{t}_{yx}=\frac{(\tau_5-\tau_1)}{\eta_1}(c_1\sin\phi-c_2\cos\phi)=0. \tag{3.1.10}$$

Integrating with respect to ϕ gives

$$W=\tfrac{1}{2}K_2^c\left(\frac{d\phi}{dz}\right)^2=-K_2^c\frac{\eta_0}{\eta_1}(c_1\cos\phi+c_2\sin\phi)+\text{constant}, \tag{3.1.11}$$

where we have introduced the constant

$$\eta_0=\frac{(\tau_5-\tau_1)}{K_2^c}. \tag{3.1.12}$$

3.1.4. *The viscous dissipation inequality*

The following thermodynamic relation constrains the magnitude of the viscosity coefficients

$$\eta_1\left[\left(\frac{du}{dz}\right)^2+\left(\frac{dv}{dz}\right)^2\right]+\eta_2\left[\frac{du}{dz}\cos\phi+\frac{dv}{dz}\sin\phi\right]^2\geqslant 0, \tag{3.1.13}$$

or, using equations (3.1.5) and (3.1.6)

$$c_1\frac{du}{dz}+c_2\frac{dv}{dz}\geqslant 0. \tag{3.1.14}$$

To learn some more about the viscosity combinations relevant to this problem, η_i, we look at the viscosity experiments carried out by Miesowicz [10] on nematics. Miesowicz oriented the sample by applying a strong magnetic field and then measured the apparent viscosity η for different director geometries where

$$\eta=\frac{\text{shear stress}}{\text{velocity gradient}}=\frac{\tilde{t}_{ji}}{2D_{ij}}. \tag{3.1.15}$$

When the flow is confined to the plane of shear (i.e. $v(z)=0$) and the c director is fixed parallel to this flow (i.e. $\phi=0$) then equation (3.1.5) yields

$$\tilde{t}_{xz}=(\eta_1+\eta_2)\frac{du}{dz}=c_1 \tag{3.1.16}$$

and hence, using equations (3.1.14) and (3.1.15), the apparent viscosity for the c director aligned parallel to the flow is

$$\eta_{\mathrm{pl}}=(\eta_1+\eta_2)\geqslant 0. \qquad (3.1.17)$$

Similarly when the c director is fixed perpendicular to the plane of shear (i.e. $\phi=\frac{1}{2}\pi$), equation (3.1.5) yields

$$\tilde{t}_{xz}=\eta_1\frac{du}{dz}=c_1 \qquad (3.1.18)$$

and hence, using equations (3.1.14) and (3.1.15) again, the apparent viscosity for the c director aligned perpendicular to the flow is

$$\eta_{\mathrm{pd}}=\eta_1\geqslant 0. \qquad (3.1.19)$$

Since results from experiments such as these for smectics are not known at this time it seems that our best approximations for the η_i can be achieved by looking at the similar coefficients derived from tests like these for nematics. Typical values are roughly $\eta_{\mathrm{pl}}=0{\cdot}02$ p and $\eta_{\mathrm{pd}}=0{\cdot}03$ p which suggest for purposes of illustration that we should take $\eta_1=3\eta_0$ and $\eta_2=-\eta_0$.

3.1.5. *The Lagrange multipliers, β_i*

The Lagrange multipliers are thought to be couples that are inherent in the layered structure of the smectic materials, which resist destabilising forces on the layers that occur when an external stimulus is applied, and hence allow the initial static geometry to be preserved under such disturbances.

It is therefore of importance to discover the form that these multiplers take if not only to discover whether the fixed parallel layer assumption is feasible but also to perhaps shed some light on their behaviour and role. From the angular momentum a equations we obtain

$$\boldsymbol{\beta}=[-\beta_1(z),\beta_2(z),0], \qquad (3.1.20)$$

where

$$\left.\begin{aligned}\frac{d\beta_1}{dz}&=\tilde{t}_{yz}-\tilde{t}_{zy}+K_4^c\left(\frac{d\phi}{dz}\right)^2\sin\phi=(\lambda_4-\lambda_1)\frac{dv}{dz}+\sigma(z)\sin\phi,\\ \frac{d\beta_2}{dz}&=\tilde{t}_{xz}-\tilde{t}_{zx}+K_4^c\left(\frac{d\phi}{dz}\right)^2\cos\phi=(\lambda_4-\lambda_1)\frac{du}{dz}+\sigma(z)\cos\phi,\end{aligned}\right\} \qquad (3.1.21)$$

and

$$\sigma(z)=(\lambda_2-\lambda_3+\lambda_5+\lambda_6)\left(\frac{du}{dz}\cos\phi+\frac{dv}{dz}\sin\phi\right)+K_4^c\left(\frac{d\phi}{dz}\right)^2. \qquad (3.1.22)$$

Therefore the existence of a finite solution for these multipliers suggests that the planar homeotropic arrangement is stable under a finite shear parallel to the layers for any surface alignment.

3.1.6. *Scaling analysis*

For a more general discussion of this problem we adopt the following scaling first introduced by Ericksen [11]

$$\bar{z}=\frac{z}{d},\quad \bar{v}=vd,\quad \bar{c}=cd^2, \qquad (3.1.23)$$

where v represents either of the velocity components u or v, and c denotes either of the shear forces c_1 or c_2. Substituting equations (3.1.23) into equations (3.1.7) and (3.1.8) we obtain

$$\left.\begin{aligned}\frac{d\bar{u}}{d\bar{z}}&=\frac{\bar{c}_1(\eta_1+\eta_2\sin^2\phi)-\bar{c}_2\eta_2\sin\phi\cos\phi}{\eta_1(\eta_1+\eta_2)},\\ \frac{d\bar{v}}{d\bar{z}}&=\frac{\bar{c}_2(\eta_1+\eta_2\cos^2\phi)-\bar{c}_1\eta_2\sin\phi\cos\phi}{\eta_1(\eta_1+\eta_2)},\end{aligned}\right\} \qquad (3.1.24)$$

and equation (3.1.11) becomes

$$=\left(\frac{d\phi}{d\bar{z}}\right)^2=-2\frac{\eta_0}{\eta_1}(\bar{c}_1\cos\phi+\bar{c}_2\sin\phi)+\text{constant} \qquad (3.1.25)$$

which gives us a neat summary of the problem.

3.1.7. *Equilibrium analysis*

To investigate the stability of the flow we look at a time dependent director profile and a simple newtonian linear velocity profile and assume that no secondary velocity is evident at flow alignment.

$$\mathbf{a}=[0,0,1],\quad \mathbf{c}=[\cos\phi(t),\sin\phi(t),0],\quad \mathbf{v}=[kz,0,0], \qquad (3.1.26)$$

where k is a positive constant. In this event the angular momentum equations reduce to

$$2\lambda_5\frac{d\phi}{dt}+k(\tau_5-\tau_1)\sin\phi=0, \qquad (3.1.27)$$

where the dissipation inequality implies that λ_5 is positive. It follows that the director tends towards some fixed alignment angle given by

$$\phi\to 0 \text{ if } \tau_5>\tau_1 \quad\text{and}\quad \phi\to\pi \quad\text{if}\quad \tau_1>\tau_5. \qquad (3.1.28)$$

Intuitively it seems natural that the c director will align with the flow ($\phi=0$) rather than against it ($\phi=\pi$). Therefore it seems reasonable to assume that τ_5 is greater than τ_1.

3.1.8 *The general solution for asymmetric boundary conditions*

In this case a twisted smectic or a chiral smectic is assumed to have a surface alignment on the lower plate that is the opposite of that on the upper one. Therefore we allow the director profile $\phi(z)$ to be represented by a function that is asymmetric about the flow alignment angle $\phi=0$ and has the following boundary conditions

$$\left.\begin{aligned}\phi(-1)&=-\phi_0, & \bar{u}(-1)&=0, & \bar{v}(-1)&=0,\\ \phi(1)&=+\phi_0, & \bar{u}(1)&=\bar{U}, & \bar{v}(1)&=0,\end{aligned}\right\} \qquad (3.1.29)$$

where ϕ_0 and $\bar{U}$ are positive constants and strong anchoring is assumed. The director is odd in z so

$$\phi(-\bar{z})=-\phi(\bar{z}). \qquad (3.1.30)$$

Let us introduce the rate of change of ϕ at the middle of the sample defined by

$$\left.\frac{d\phi}{d\bar{z}}\right|_{\bar{z}=0}=\phi'_{\mathrm{m}}. \qquad (3.1.31)$$

This input variable represents the magnitude of the applied shear and, due to flow alignment considerations, must satisfy the constraint

$$\phi'_{\mathrm{m}} < \phi_0. \tag{3.1.32}$$

Substituting equation (3.1.30) into equation (3.1.25) and resolving into its even components

$$\left(\frac{d\phi}{d\bar{z}}\right)^2 = -2\frac{\eta_0}{\eta_1}\bar{c}_1 \cos\phi + \text{constant} \tag{3.1.33}$$

and its odd components

$$0 = -2\frac{\eta_0}{\eta_1}\bar{c}_2 \sin\phi \tag{3.1.34}$$

the latter of which implies that

$$\bar{c}_2 = 0. \tag{3.1.35}$$

Upon introduction of equation (3.1.31) into equation (3.1.33) we obtain

$$\left(\frac{d\phi}{d\bar{z}}\right)^2 = 2\frac{\eta_0}{\eta_1}\bar{c}_1(1-\cos\phi) + \phi'^2_{\mathrm{m}}, \tag{3.1.36}$$

which can be rearranged and integrated with respect to $\bar{z}$ from $\bar{z}=0$ to $\bar{z}=1$

$$1 = \int_0^{\phi_0} \frac{\eta_1^{1/2}}{[2\eta_0\bar{c}_1(1-\cos\phi) + \eta_1\phi'^2_{\mathrm{m}}]^{1/2}}\, d\phi, \tag{3.1.37}$$

yielding $\bar{c}_1$ for a certain ϕ_0 and ϕ'_{m}. Similarly this gives an expression for the director profile

$$\bar{z}(\phi) = \int_0^{\phi} \frac{\eta_1^{1/2}}{[2\eta_0\bar{c}_1(1-\cos\phi) + \eta_1\phi'^2_{\mathrm{m}}]^{1/2}}\, d\phi. \tag{3.1.38}$$

From equations (3.1.24) (3.1.35) and (3.1.36) the velocity components are

$$\left.\begin{aligned} \bar{u}(\bar{z}) &= \frac{\bar{c}_1}{\eta_1^{1/2}(\eta_1+\eta_2)} \int_{-\phi_0}^{\phi} \frac{\eta_1 + \eta_2\sin^2\phi}{[2\eta_0\bar{c}_1(1-\cos\phi) + \eta_1\phi'^2_{\mathrm{m}}]^{1/2}}\, d\phi, \\ \bar{v}(\bar{z}) &= \frac{-\bar{c}_1}{\eta_1^{1/2}(\eta_1+\eta_2)} \int_{-\phi_0}^{\phi} \frac{\eta_2\sin\phi\cos\phi}{[2\eta_0\bar{c}_1(1-\cos\phi) + \eta_1\phi'^2_{\mathrm{m}}]^{1/2}}\, d\phi \end{aligned}\right\} \tag{3.1.39}$$

and therefore

$$\bar{U} = \frac{2\bar{c}_1}{\eta_1^{1/2}(\eta_1+\eta_2)} \int_0^{\phi_0} \frac{\eta_1 + \eta_2\sin^2\phi}{[2\eta_0\bar{c}_1(1-\cos\phi) + \eta_1\phi'^2_{\mathrm{m}}]^{1/2}}\, d\phi. \tag{3.1.40}$$

The boundary condition $\bar{v}(1)$ equal to zero is automatically satisfied, as the integrand is an odd function calculated over a symmetrical range. These integrals cannot be evaluated analytically but they can all be written in terms of the incomplete elliptical integrals of the first and second kind which can be calculated quickly and precisely using mathematical packages.

3.1.9. *Numerical results for asymmetric boundary conditions*

For all calculations we take η_0 equal to unity since it is only a scaling parameter and does not affect the form of the output. Initially we consider a cell in which the alignment at the lower surface is parallel but opposite to that on the upper one, i.e. there is a complete twist of 2π across the cell. Figure 1 (*a*) simply illustrates the fact that the director profile becomes flatter, and therefore increasingly oriented towards the flow alignment angle, as the applied shear is increased. Figure 1 (*b*) shows that the in-plane velocity is fairly linear with only a few small undulations corresponding to the interaction with the distortions of the director. Of most interest is the transverse velocity component, in figure 1 (*c*), which is seen to change sign twice across the sample. As the applied velocity rises the bulk of the secondary velocity occupies the middle of the cell with the areas of fluctuation being increasingly confined to the boundaries.

The evolution of the system as the shear rate rises is illustrated in figure 2. Figure 2 (*a*) shows that the smectic is relatively easy to deform initially but this process gets harder and harder as the majority of the sample becomes oriented at the flow alignment angle. The transverse velocity as a proportion of the in-plane velocity, figure 2 (*b*), is seen to tend towards a limit as the applied shear increases. It is also found that the shearing force per unit area c_1 increases almost linearly with $\bar{U}$.

Expanding the number of twists in the smectic helix as we cross the cell from one to six illustrates the type of behaviour we could expect from shear flow of chiral smectic C*. Figure 3 (*a*) shows that for small shear rates the director orients at the flow alignment angle quite evenly across the sample. But as the shear rate rises the untwisting of the helix becomes confined to a small boundary layer. The strong anchoring assumed at the boundary would probably not be evident in these areas of high distortion and some relaxation must take place. The in-plane velocity profiles are all approximately linear at these large shear rates but examination of the transverse velocity profiles, in figure 3 (*b*), again illustrates that the areas of fluctuation correspond to the regions of untwisting.

3.1.10. *Numerical results for symmetric boundary conditions*

The asymmetric surface geometry was investigated because it not only simplified the analysis of the problem but it was also readily adapted to illustrate the behaviour of chiral and achiral smectics. However, the general case can be numerically modelled in a similar way and to demonstrate the effect of different surface alignments we select

$$\left.\begin{aligned}\phi(-1)&=+\phi_0, & \bar{u}(-1)&=0, & \bar{v}(-1)&=0,\\ \phi(1)&=+\phi_0, & \bar{u}(1)&=\bar{U}, & \bar{v}(1)&=0\end{aligned}\right\} \tag{3.1.41}$$

which define a symmetric director profile. For symmetric boundary conditions ϕ'_m is always zero so the driving variable must be altered. We choose ϕ_m, the maximum distortion of the director from its surface orientation, defined by

$$\phi_m=\phi(0). \tag{3.1.42}$$

Unlike the asymmetric case $\bar{c}_2$ is non-zero. In figure 4 the surface orientation is taken to be aligned against the flow but slightly out of the plane of shear as the director must be perturbed from this unstable equilibrium position (see § 3.1.7) for non-trivial results. Figure 4 (*a*) illustrates how the director rotates into the plane of shear as the velocity now has an odd profile to complement the evenness of the director profile. The in-plane velocity component is fairly linear and similar to its asymmetric counterpart shown in figure 1 (*b*).

In figure 5 (*a*) it is seen that when the *c* director is initially pointing against the applied shear (solid line) it takes a relatively large velocity for a small initial movement of the *c* director. Above a certain velocity, however, the molecules lie sufficiently out of

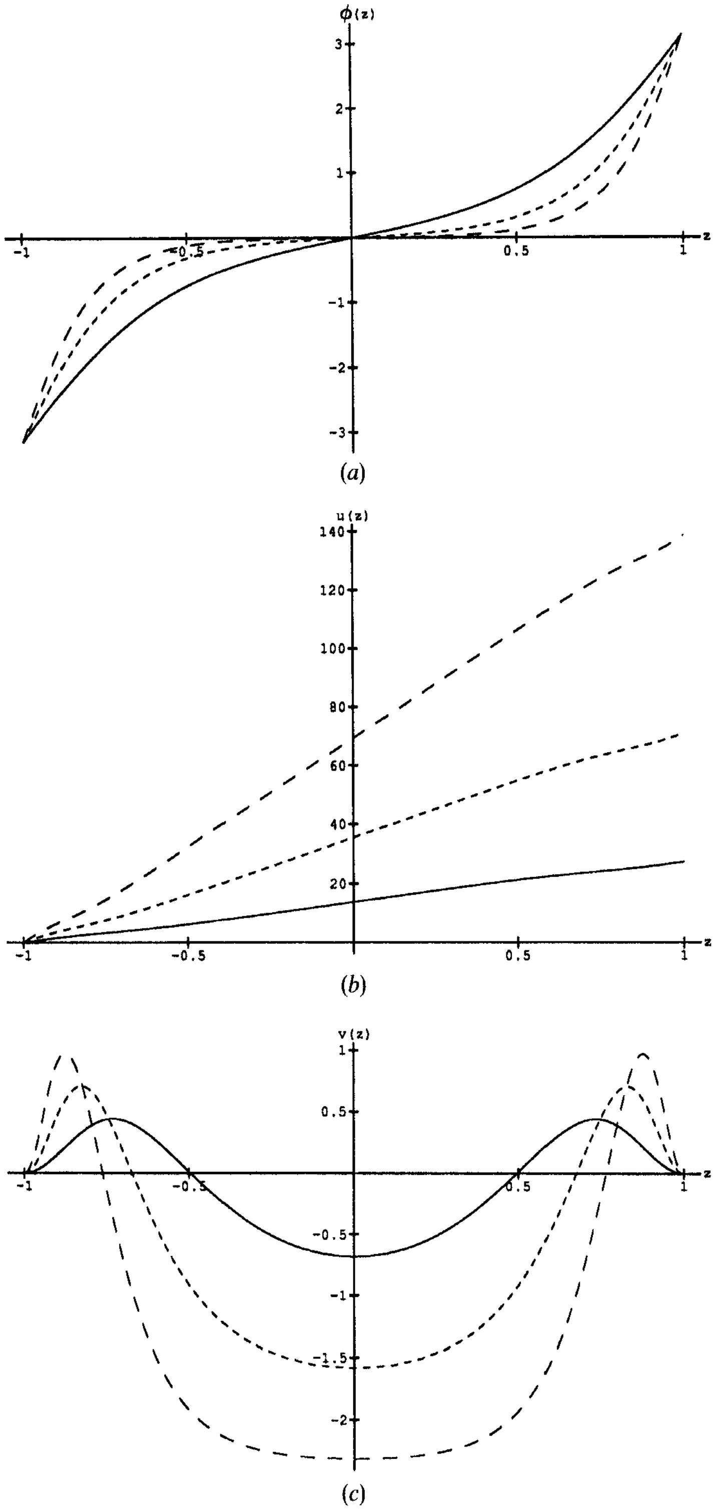

Figure 1. Cross-cell profiles for (a) $\phi(\bar{z})$, (b) $\bar{u}(\bar{z})$ and (c) $\bar{v}(\bar{z})$ for $\phi_0=\pi$ and $\phi'_m=1{\cdot}00$ (solid line), $\phi'_m=0{\cdot}25$ (dotted line) and $\phi'_m=0{\cdot}05$ (dashed line).

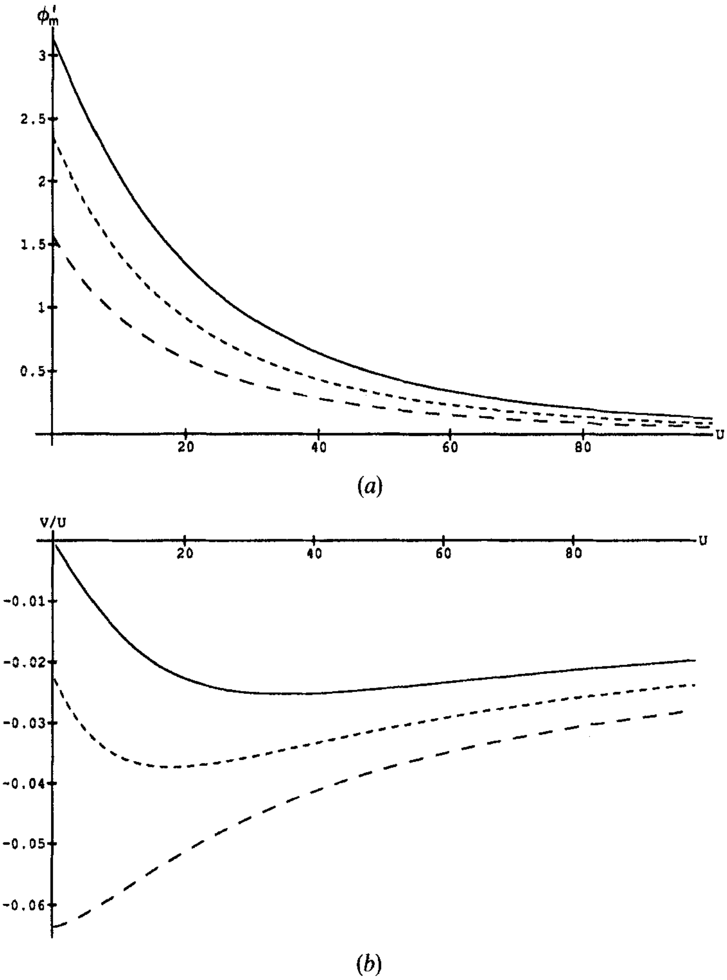

Figure 2. Illustration of (a) ϕ_m' and (b) $\bar{V}/\bar{U}$, where $\bar{V}$ is the maximum value of $\bar{v}/(\bar{z})$, as functions of the applied velocity $\bar{U}$ for $\phi_0=\pi$ (solid line), $\phi_0=\frac{3}{4}\pi$ (dotted line) and $\phi_0=\frac{1}{2}\pi$ (dashed line).

the plane of shear to be easily oriented towards the direction of flow. Although $\bar{c}_1$ increases fairly linearly with $\bar{U}$ the shearing force per unit area in the y direction exhibits some interesting behaviour. It is shown in figure 5 (b) that the transverse shear component is nearly zero when the c director is aligned against the flow but this greatly increases when the director profile starts to be distorted. It then decreases as the molecules begin to rotate round to orient with the flow and eventually changes sign and becomes linear in $\bar{U}$ when the bulk of the sample has reached flow equilibrium.

3.2. *Shear flow of smectics C_M and C_M^**

3.2.1. *The governing equations*

For this degenerate case of the previous shear situation we simply put all the coefficients of the constitutive terms that contain odd multiples of **a** and **c** (see

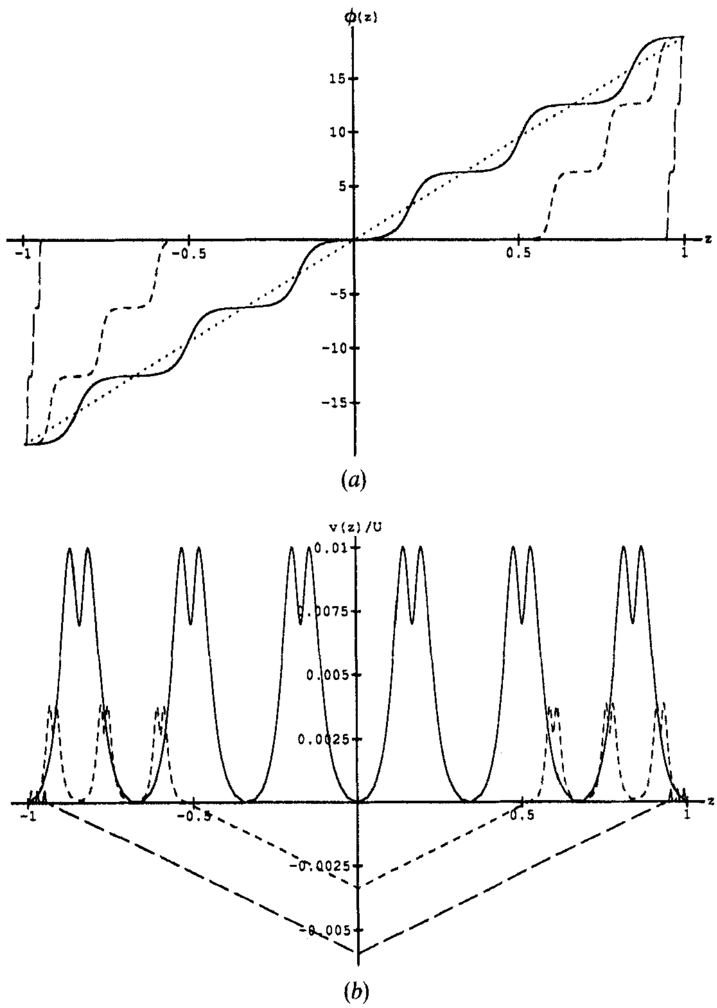

Figure 3. Cross-cell profiles for (*a*) $\phi(\bar{z})$ and (*b*) $\bar{v}(\bar{z})$ for $\phi_0 = 6\pi$ and $\phi'_m = 1{\cdot}00$ (solid line), $\phi'_m = 0{\cdot}035$ (dotted line) and $\phi'_m = 0{\cdot}02$ (dashed line) corresponding to $\bar{U} \approx 1{\cdot}5$, 11 and 700 ($\times 10^3$). The straight, dotted line represents the undisturbed alignment.

equation (2.3)) to zero. We find that the governing equation (3.1.24) remains unchanged and equation (3.1.25) becomes

$$\left(\frac{d\phi}{d\bar{z}}\right)^2 = \text{constant}. \tag{3.2.1}$$

Due to the absence of any viscous torques in equation (3.2.1) it is obvious that the director profile $\phi(z)$ will be a linear function of z prescribed by the director surface orientations. Therefore no flow alignment can be possible.

3.2.2. *The general solution for asymmetric boundary conditions*

Employing the same boundary conditions as described by equations (3.1.29) we find that equation (3.2.1) implies a linear director profile across the cell

$$\phi(\bar{z}) = \phi_0 \bar{z} \tag{3.2.2}$$

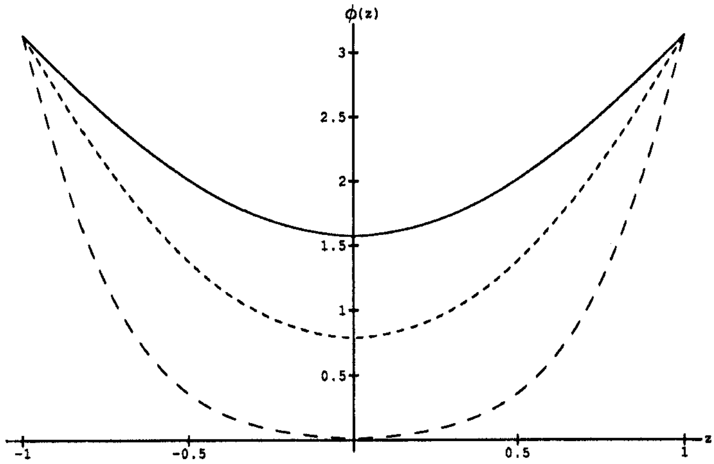

(a)

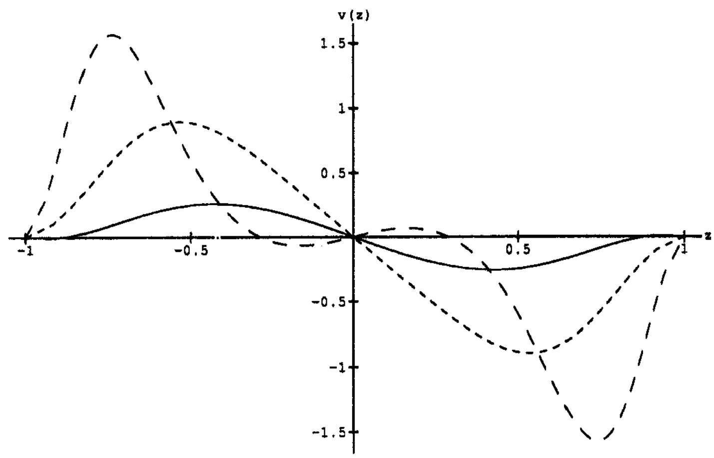

(b)

Figure 4. Cross-cell profiles for (a) $\phi(\bar{z})$, (b) $\bar{v}(\bar{z})$ for $\phi_0=3{\cdot}14$ and $\phi_m=\frac{1}{2}\pi$ (solid line), $\phi_m=\frac{1}{4}\pi$ (dotted line) and $\phi_m=0{\cdot}01$ (dashed line).

and so, assuming that ϕ_0 is non-zero, equations (3.1.24) can be integrated with respect to $\bar{z}$ to give

$$\left.\begin{aligned}\bar{u}(\bar{z})&=\frac{\bar{U}[(2\eta_1+\eta_2)(\bar{z}+1)-\eta_2(p(\bar{z})+p(1))]}{2[2\eta_1+\eta_2(1-p(1))]},\\ \bar{v}(\bar{z})&=\frac{\bar{U}\eta_2[q(\bar{z})-q(1)]}{2[2\eta_1+\eta_2(1-p(1))]},\end{aligned}\right\}\qquad(3.2.3)$$

where

$$\left.\begin{aligned}p(\bar{z})&=\frac{\sin(2\phi_0\bar{z})}{2\phi_0},\\ q(\bar{z})&=\frac{\cos(2\phi_0\bar{z})}{2\phi_0},\end{aligned}\right\}\qquad(3.2.4)$$

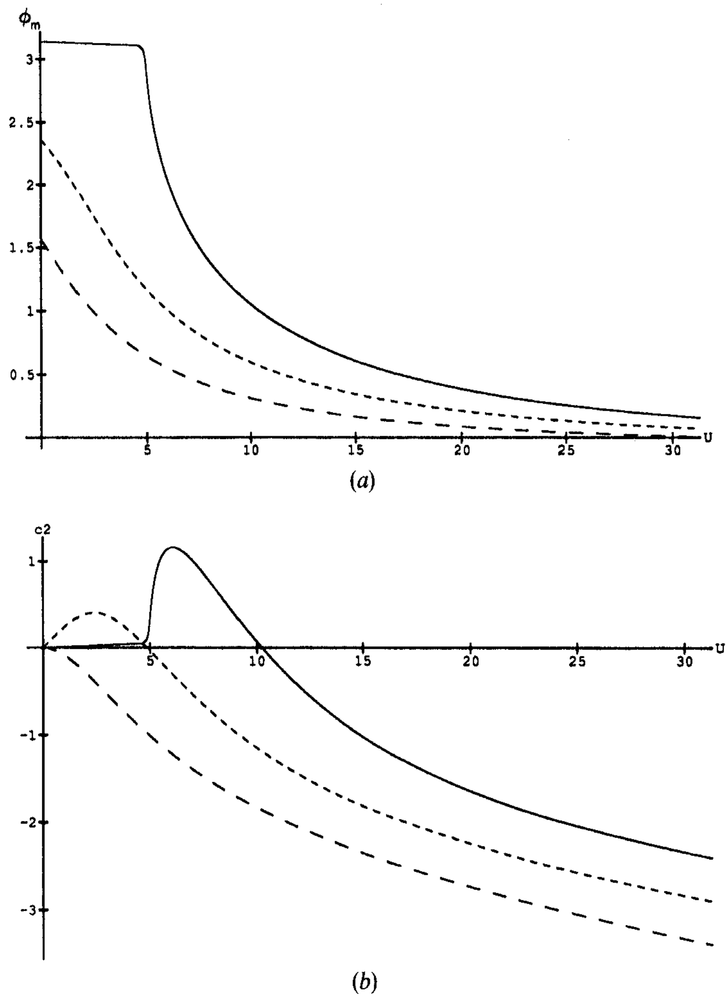

Figure 5. Illustration of (*a*) ϕ_m and (*b*) $\bar{c}_2$ as functions of the applied velocity $\bar{U}$ for $\phi_0 = 3{\cdot}14$ (solid line), $\phi_0 = \frac{3}{4}\pi$ (dotted line) and $\phi_0 = \frac{1}{2}\pi$ (dashed line).

and also from equations (3.1.21) we have

$$\left.\begin{aligned}
\beta_1(\bar{z}) &= \frac{\eta_2(\lambda_4-\lambda_1)-\eta_1(\lambda_2-\lambda_3+\lambda_5+\lambda_6)}{\eta_2}\,\bar{v}(\bar{z}),\\
\beta_2(\bar{z}) &= \frac{\eta_2(\lambda_4-\lambda_1)-\eta_1(\lambda_2-\lambda_3+\lambda_5+\lambda_6)}{\eta_2}\,\bar{u}(\bar{z})\\
&\quad +(\lambda_2-\lambda_3+\lambda_5+\lambda_6)\frac{\bar{U}\eta_1(\eta_1+\eta_2)(\bar{z}+1)}{\eta_2[2\eta_1+\eta_2(1-p(1))]}.
\end{aligned}\right\} \qquad (3.2.5)$$

3.2.3. *Discussion of results for asymmetric boundary conditions*

As the director profile is linear and pre-determined by the boundary conditions it is clear that no flow alignment will occur. The in-plane velocity is almost linear in $\bar{z}$ with small sinusoidal fluctuations corresponding to the regular sinusoidal oscillations of the transverse velocity component.

4. Shear flow of a bookshelf sample

The sample is arranged in vertical layers between two infinite horizontal parallel plates a distance $2d$ apart (Beresnev *et al.* [8]). The lower one is at rest while the upper one is moved parallel to the layers with a velocity U in a straight line in its own plane. The alignment is described by the layer normal **a** which coincides with the y axis and the projection of the director in the shear plane **c**.

Therefore the velocity and the director orientation are described by

$$\mathbf{a}=[0,1,0], \quad \mathbf{c}=[\cos\phi(z),0,\sin\phi(z)], \quad \mathbf{v}=[u(z),v(z),0],$$

where ϕ is the angle between **c** and the x axis, $u(z)$ is the velocity in the shear plane and $v(z)$ is a secondary velocity component.

The chirality of the helical phases means that the director rotates as we progress along the layer normal and so the system variables must be dependent on the lateral variable y. In this case the conflict between the twisted structure and the planar boundaries leads to the formation of line disinclinations [12]. The dynamics of such a system, however, are beyond the scope of the present study and so are not discussed here.

4.1. *Shear flow of smectic C*

4.1.1. *The elastic energy function*

The elastic deformations are only due to the rotation of the c director by moving the layers parallel or perpendicular to it and so

$$W=\tfrac{1}{2}(K_2^c+K_3^c)(\mathbf{a}\cdot\nabla\times\mathbf{c})^2+\tfrac{1}{2}(K_1^c+K_2^c)(\nabla\cdot\mathbf{c})^2=\tfrac{1}{2}f(\phi)\left(\frac{d\phi}{dz}\right)^2, \tag{4.1.1}$$

where

$$f(\phi)=(K_1^c+K_2^c)\cos^2\phi+(K_2^c+K_3^c)\sin^2\phi. \tag{4.1.2}$$

Discussion of these static coefficients [9] suggests that $K_1^c+K_2^c$ and $K_2^c+K_3^c$ are positive.

4.1.2. *The linear momentum balance*

In the absence of applied pressure gradients, external body forces and couples and using the Onsager relations we have

$$\left.\begin{aligned}\frac{d(\tilde{t}_{xz})}{dz}&=\frac{d}{dz}\left[\xi_1(\phi)\frac{du}{dz}+\xi_2(\phi)\frac{dv}{dz}\cos\phi\right]=0,\\ \frac{d(\tilde{t}_{yz})}{dz}&=\frac{d}{dz}\left[\xi_3(\phi)\frac{dv}{dz}+\xi_2(\phi)\frac{du}{dz}\cos\phi\right]=0\end{aligned}\right\} \tag{4.1.3}$$

in the x and y directions, respectively, where the functions $\xi_i(\phi)$ are given by

$$\left.\begin{aligned}\xi_1(\phi)&=\tfrac{1}{2}(\mu_0+\mu_4+\lambda_5)+\lambda_2\cos 2\phi+\mu_3\sin^2\phi\cos^2\phi,\\ \xi_2(\phi)&=\tfrac{1}{2}(\kappa_1+\tau_1+\tau_2+\tau_5)+(\kappa_3+\tau_4)\sin^2\phi,\\ \xi_3(\phi)&=\tfrac{1}{2}(\mu_0+\mu_2+2\lambda_1+\lambda_4)\\ &\quad+\tfrac{1}{2}(\mu_4+\mu_5-2\lambda_2+2\lambda_3+\lambda_5+\lambda_6)\sin^2\phi\end{aligned}\right\} \tag{4.1.4}$$

and so the velocity components are given by

$$\left.\begin{aligned}\frac{du}{dz}&=\frac{c_2\xi_2(\phi)\cos\phi-c_1\xi_3(\phi)}{\xi_2(\phi)^2\cos^2\phi-\xi_1(\phi)\xi_3(\phi)},\\ \frac{dv}{dz}&=\frac{c_1\xi_2(\phi)\cos\phi-c_2\xi_1(\phi)}{\xi_2(\phi)^2\cos^2\phi-\xi_1(\phi)\xi_3(\phi)},\end{aligned}\right\}\tag{4.1.5}$$

where c_1 and c_2 are constants of integration and are the shearing forces per unit area in the x and y directions.

4.1.3. *The angular momentum balance*

From the angular momentum c equations we have

$$f(\phi)\frac{d^2\phi}{dz^2}+\tfrac{1}{2}f'(\phi)\left(\frac{d\phi}{dz}\right)^2-(\lambda_5+\lambda_2\cos 2\phi)\frac{du}{dz}-(\tau_1+\tau_5)\frac{dv}{dz}\cos\phi=0,\tag{4.1.6}$$

or, substituting equations (4.1.1) and (4.1.5) we obtain

$$\frac{dW}{d\phi}=\tilde{t}_{xz}-\tilde{t}_{zx}=c_1f_1(\phi)+c_2f_2(\phi),$$

where

$$\left.\begin{aligned}f_1(\phi)&=\frac{(\tau_1+\tau_5)\xi_2(\phi)\cos^2\phi-(\lambda_5+\lambda_2\cos 2\phi)\xi_3(\phi)}{\xi_2(\phi)^2\cos^2\phi-\xi_1(\phi)\xi_3(\phi)},\\ f_2(\phi)&=\frac{[(\lambda_5+\lambda_2\cos 2\phi)\xi_2(\phi)-(\tau_1+\tau_5)\xi_1(\phi)]\cos\phi}{\xi_2(\phi)^2\cos^2\phi-\xi_1(\phi)\xi_3(\phi)}.\end{aligned}\right\}\tag{4.1.7}$$

4.1.4. *The viscous dissipation inequality*

The following thermodynamic constraint limits the magnitude of the dissipative terms

$$\xi_1(\phi)\left(\frac{du}{dz}\right)^2+2\xi_2(\phi)\frac{du}{dz}\frac{dv}{dz}\cos\phi+\xi_3(\phi)\left(\frac{dv}{dz}\right)^2\geqslant 0,\tag{4.1.8}$$

or, employing equation (4.1.5)

$$c_1\frac{du}{dz}+c_2\frac{dv}{dz}\geqslant 0.\tag{4.1.9}$$

The general expression for the viscous dissipation inequality can be manipulated to yield

$$\xi_1(\phi)\geqslant 0,\quad\text{and}\quad \xi_3(\phi)\geqslant 0\quad\text{for all }\phi.\tag{4.1.10}$$

4.1.5. *The Lagrange multipliers, β_i*

Upon consideration of the angular momentum a equations we have to choose the β_i to depend on the lateral co-ordinate y

$$\boldsymbol{\beta}=y[\tilde{t}_{zy}-\tilde{t}_{yz}+\hat{\beta}_x,0,\tilde{t}_{yx}-\tilde{t}_{xy}+\hat{\beta}_z],\tag{4.1.11}$$

where $\hat{\beta}_x$ and $\hat{\beta}_z$ are static contributions. This implies that these inherent stabilizing couples that allow the smectic to keep its initial stratified state must increase linearly with y. This is not entirely credible, so this seems to point to the formation of some type of periodic domain structure or possibly some even more complex behaviour. The nature of this solution is not especially suprising due to the initial assumption of the action of a secondary, velocity component $v(z)$ across the layers.

4.1.6. *Equilibrium analysis*

To investigate whether any structurally stable shear situations exist let us consider the case of simple shear flow involving no transverse velocities. We allow the c-director to rely solely on time and take the velocity profile to be linear so

$$\mathbf{a}=[0,1,0], \quad \mathbf{c}=[\cos\phi(t),0,\sin\phi(t), \quad \mathbf{v}=[kz,0,0], \qquad (4.1.13)$$

where k is a positive constant. This yields the governing equation

$$2\lambda_5\frac{d\phi}{dt}+k(\lambda_5+\lambda_2\cos 2\phi)=0 \qquad (4.1.14)$$

where λ_5 is positive. It follows that the alignment of the flow depends on the relative magnitudes of λ_2 and λ_5.

If $|\lambda_2|\geqslant\lambda_5$ then we get flow alignment according to

$$\phi\to-\phi_a \text{ or } \pi-\phi_a \quad \text{if} \quad \lambda_2>0 \quad \text{and} \quad \phi\to\phi_a \text{ or } \phi_a-\pi \quad \text{if} \quad \lambda_2<0, \quad (4.1.15)$$

where ϕ_a is the acute angle satisfying

$$\cos(2\phi_a)=-\frac{\lambda_5}{\lambda_2}. \qquad (4.1.16)$$

If $|\lambda_2|<\lambda_5$ then no flow alignment can occur and a non-stationary flow develops. It would be expected that this would bear some similarity to the 'tumbling' effect exhibited by some nematic materials as described by Carlsson [13].

4.1.7. *Results for smectic C*

Unfortunately very little is known about the relative magnitudes of the nine independent viscosity coefficient combinations present in this problem and as there is no analytical solution, it is somewhat unreasonable to produce a numerical study at this stage.

4.2. *Shear flow of smectic C_M*

4.2.1. *The governing equations*

Due to the additional symmetry of the smectic C_M phase it is not necessary to introduce a secondary, velocity component into the calculation and so the remaining shear plane velocity is given by the even terms of equation (4.1.5)

$$\frac{du}{dz}=\frac{c_1}{\xi_1(\phi)} \qquad (4.2.1)$$

and the angular momentum balance, equation (4.1.6), becomes

$$f(\phi)\frac{d^2\phi}{dz^2}+\tfrac{1}{2}f'(\phi)\left(\frac{d\phi}{dz}\right)^2-(\lambda_5+\lambda_2\cos 2\phi)\frac{du}{dz}=0. \qquad (4.2.2)$$

Because of the loss of the cross-layer velocity component it is now possible to select

$$\beta=0 \qquad (4.2.3)$$

which implies the smectic structure is stable under an applied shear parallel to its layers. The long term equilibrium of the flow is similar to that for smectic C (see §4.1.6).

5. Effects of a rotating magnetic field on smectics C and C_M

Repeating analysis first applied to nematics by Tsvetkov [4] we consider the non-chiral phases' reaction to being placed in a magnetic field which rotates about the layer normal. Therefore we choose

$$\left.\begin{aligned} \mathbf{a}&=[0,0,1], & \mathbf{c}&=[\cos\phi(t),\sin\phi(t),0],\\ \mathbf{v}&=0, & \mathbf{H}&=H[\cos(\omega t),\sin(\omega t),0],\end{aligned}\right\} \tag{5.1}$$

where H is the magnitude of the magnetic field. This selection of variables assumes that the Lagrange multipliers, β_i, hold the layers parallel to the applied field. The a and c components of the magnetic body couples are given by

$$\left.\begin{aligned} G_i^a&=[\chi^a a_pH_p+\chi^{ac}c_pH_p]H_i,\\ G_i^c&=[\chi^{ac}a_pH_p+\chi^c c_pH_p]H_i,\end{aligned}\right\} \tag{5.2}$$

where χ^a and χ^c are the magnetic susceptibilities along the **a** and **c** vectors, respectively, and

$$\chi^{ac}=(\chi^a\chi^c)^{1/2}. \tag{5.3}$$

Both the smectic C and C_M phases are governed by the same equation

$$\frac{d\phi}{dt}=-\frac{\chi^cH^2}{4\lambda_5}\sin 2(\phi-\omega t), \tag{5.4}$$

which has the solution

$$\phi(t)=\begin{cases}\omega t-\tfrac{1}{2}\sin^{-1}(\omega/\omega_c) & \text{if} \quad \omega\leqslant\omega_c\\ \omega t-\dfrac{\pi}{4}-\tan^{-1}\left[\dfrac{\Omega}{(\omega+\omega_c)}\tan\left(\Omega t-\tan^{-1}\dfrac{\Omega}{(\omega-\omega_c)}\right)\right] & \text{if} \quad \omega>\omega_c,\end{cases} \tag{5.5}$$

where $\phi(0)=0$ in the latter and

$$\omega_c=\frac{\chi^cH^2}{4\lambda_5},\quad \Omega=\sqrt{(\omega^2-\omega_c^2)}. \tag{5.6}$$

Below some critical rotational velocity ω_c the c director simply rotates with the magnetic field with some constant phase lag dependent on λ_5. Above this velocity the liquid crystal exhibits more complex behaviour.

If we compare this situation with that for nematics derived by Tsvetkov for a director orientation described by $\mathbf{n}=[\cos\phi(t),\sin\phi(t),0]$

$$\frac{d\phi}{dt}=-\frac{\chi_aH^2}{2\gamma_1}\sin 2(\phi-\omega t), \tag{5.7}$$

it is remarkably similar. Although smectics are much more complicated than a two dimensional nematic it appears that they behave like one when the magnetic field is in the plane of the layers.

6. Unwinding the chiral helix of smectics C* and C_M^* with a magnetic field

As a magnetic field is applied parallel to the layers of a chiral smectic liquid crystal the effect on the helix as the field is increased is investigated. Therefore, assuming the layers remain parallel to the field, we have

$$\mathbf{a}=[0,0,1], \quad \mathbf{c}=[\cos\phi(z),\sin\phi(z),0], \quad \mathbf{v}=0, \quad \mathbf{H}=[H,0,0], \tag{6.1}$$

which yields the following governing equation for both smectics C* and C_M^*

$$K_2^c\frac{d^2\phi}{dz^2}=\chi^c H^2\sin\phi\cos\phi. \tag{6.2}$$

This implies that the critical field at which the helix is totally unwound is given by

$$H_c=\frac{\pi^2}{P}\left(\frac{K_2^c}{\chi^c}\right)^{1/2}, \tag{6.3}$$

where P is the pitch.

When compared with the analysis of de Gennes [5] and Meyer [6] for cholesterics for a director in the plane of the field, i.e. $\mathbf{n}=[\cos\phi)(z),\sin\phi(z),0]$

$$K_2\frac{d^2\phi}{dz^2}=\chi_a H^2\sin\phi\cos\phi \tag{6.4}$$

the similarity is clear. This leads us to the conclusion that in this one simple situation a chiral smectic phase behaves as a two-dimensional cholesteric.

References

[1] LESLIE, F. M., STEWART, I. W., and NAKAGAWA, M., 1991, *Molec. Crystals liq. Crystals*, **198,** 443.
[2] CARLSSON, T., STEWART, I. W., and LESLIE, F. M., 1992, *J. Phys.* A, **25,** 2371.
[3] BRAND, H. R., and PLEINER, H., 1991, *J. Phys., France*, **1,** 1455.
[4] TSVETKOV, V., 1939, *Acta physicochim (USSR)*, **10,** 557.
[5] DE GENNES, P. G., 1968, *Solid St. Commun.*, **6,** 163.
[6] MEYER, R. B., 1968, *Appl. Phys. Lett.*, **12,** 281.
[7] LESLIE, F. M., STEWART, I. W., CARLSSON, T., and NAKAGAWA, M., 1991, *Continuum Mech. Thermodyn.*, **3,** 237.
[8] BERESNEV, L. A., BLINOV, L. M., OSIPOV, M. A., and PIKIN, S. A., 1988, *Molec. Crystals liq. Crystals* A, **158,** 3.
[9] CARLSSON, T., STEWART, I. W., and LESLIE, F. M., 1991, *Liq. Crystals*, **9,** 661.
[10] MIESOWICZ, M., 1946, *Nature, Lond.*, **158,** 27.
[11] ERICKSEN, J. L., 1969, *Trans. Soc. Rheol.*, **13,** 9.
[12] GLOGAROVA, M., FOUSEK, J., LEJCEK, L., and PAVEL, J., 1984, *Ferroelectrics*, **58,** 161.
[13] CARLSSON, T., 1984, *Molec. Crystals liq. Crystals*, **104,** 307.